ELSEVIER

A wireless batch sealed absolute capacitive pressure sensor

Orhan Akar[b], Tayfun Akin[a,b,*], Khalil Najafi[c]

[a]*Department of Electrical and Electronics Engineering, Middle East Technical University, 06531 Ankara, Turkey*
[b]*TUBITAK-BILTEN, Middle East Technical University, Ankara, Turkey*
[c]*Center for Wireless Integrated Microsystems, The University of Michigan, Ann Arbor, MI, USA*

Abstract

This paper reports the development of an absolute wireless pressure sensor that consists of a capacitive sensor and a gold-electroplated planar coil. Applied pressure deflects a 6 μm-thin silicon diaphragm, changing the capacitance formed between it and a metal electrode supported on a glass substrate. The resonant frequency of the LC circuit formed by the capacitor and the inductor changes as the capacitance changes; this change is sensed remotely through inductive coupling, eliminating the need for wire connection or implanted telemetry circuits. The sensor is fabricated using the dissolved-wafer process and utilizes a boron-doped silicon diaphragm supported on an insulating glass substrate. The complete sensor measures 2.6 mm × 1.6 mm in size and incorporates a 24-turns gold-electroplated coil that has a measured inductance of 1.2 μH. The sensor is designed to provide a resonant frequency change in the range 95–103 MHz for a pressure change in the range 0–50 mmHg with respect to ambient pressure, providing a pressure responsivity and sensitivity of 160 kHz/mmHg and 1553 ppm/mmHg, respectively. The measured pressure responsivity and sensitivity of the fabricated device are 120 kHz/mmHg and 1579 ppm/mmHg, respectively. © 2001 Elsevier Science B.V. All rights reserved.

Keywords: Wireless sensor; Sealed pressure sensor; Capacitive pressure sensor

1. Introduction

Absolute pressure sensors are required in many applications, including industrial process control, environmental monitoring, and biomedical systems. Capacitive pressure sensors provide very high pressure sensitivity, low noise, and low temperature sensitivity and are preferred in many emerging high-performance applications. However, to fabricate absolute pressure sensors with sealed cavities that also allow easy lead transfer from inside of the cavity to outside requires relatively complex fabrication technologies [1]. In addition to the need for batch-sealed absolute pressure sensors, many emerging applications require these sensors to operate via a wireless link. One such application is in continuous long-term monitoring of the pressure for various medical applications [2]. Some wireless telemetry systems use active transmitters, however, these devices are often big and require a power source in the form of an implanted battery, or an implanted active circuit that can receive power through inductive telemetry [3]. Both of these complicate the system design and operation.

This paper presents a new structure for wireless absolute capacitive pressure sensors. The structure utilizes a parallel capacitor–inductor resonant circuit. The capacitor is formed by the pressure sensor and changes in response to changes in pressure. The on-chip inductor is fabricated inside the sealed cavity of the sensor and is connected to the pressure sensitive capacitor. Because the inductor is inside the sealed cavity of the pressure sensor, lead transfer outside of the cavity is not needed, which in turn allows one to batch seal pressure sensors at the wafer level. Furthermore, the sensor can be operated using a passive telemetry approach [4–8], as discussed in Section 3. Section 4 summarizes the fabrication process, and Section 5 presents fabrication and test results.

2. Sensor structure

Fig. 1 shows the structure of the wireless pressure sensor. It consists of a boron-doped silicon diaphragm with a thickness of ∼3–6 μm, which is supported by anchors that fix it to a glass substrate. The diaphragm is suspended over the glass by a gap of about 2 μm and can deflect when the pressure across it changes, forming a variable-gap capacitor. To obtain high pressure sensitivity, the capacitive gap should be as small as possible, usually in the range of 1–2 μm.

* Corresponding author. Tel.: +90-312-2102369;
fax: +90-312-2101261.
E-mail address: tayfun-akin@metu.edu.tr (T. Akin).

Nomenclature

A	constant determined by the ratio of (d/D) [9]
B	constant determined by number of turns in coil [9]
d	cross-sectional diameter of an individual coil winding (in.)
D	line space plus line width (in.)
g	$\sqrt{s_1^2 + s_2^2}$
L_0	inductance of a planar rectangular coil (μH)
N	number of turns
s_1	average length of side 1 of the coil (in.)
s_2	average length of side 2 of the coil (in.)

The capacitor gap should also house the gold-electroplated coil. The planar coil is placed in a recessed glass area around the metal capacitor plate on the glass. By making the recess as deep as possible, it is possible to fabricate very thick on-chip coils with high Q. This is necessary to obtain high sensitivity for the sensor. Fig. 2 shows the cross-section and electrical equivalent circuit of the wireless pressure sensor. The variable capacitor and the electroplated coil inside the sensor form a LC circuit, whose resonant frequency changes with the applied pressure. The change in the resonant frequency is sensed remotely using inductive coupling, eliminating the need for wire connection to monitor the applied pressure. The following section presents an overview of the inductive coupling link and requirements for remote signal detection.

3. Inductive coupling link

Fig. 3 shows the equivalent circuit model of the inductive coupling link used in the telemetric readout. The sensor is modeled with an inductor, L_S, a series resistance of the
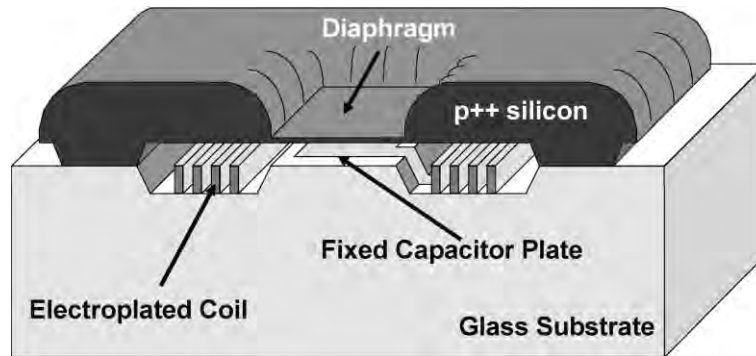

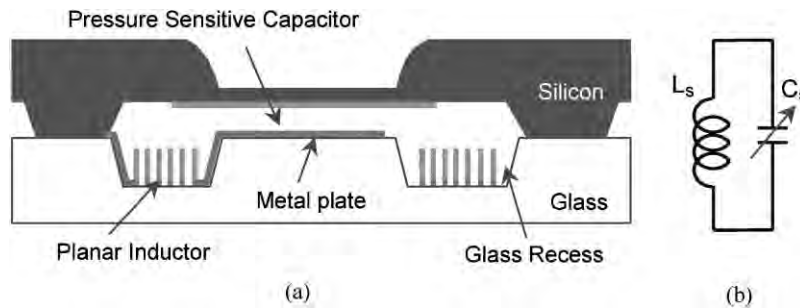Fig. 1. Structure of the wireless pressure sensor.

Fig. 2. Wireless capacitive pressure sensor: (a) cross-section; (b) electrical equivalent circuit. The change in the resonance frequency due to capacitance change is sensed remotely using inductive coupling, eliminating the need for wire connection.
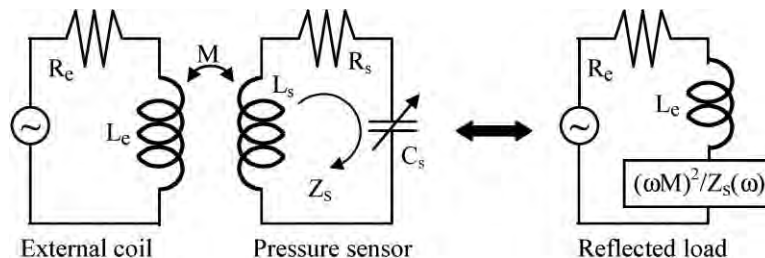

Fig. 3. Equivalent circuit model of the telemetric readout approach.

inductor, R_S, and a variable capacitor, C_S. The resonance frequency of the sensor is given by

$$f_0 = \frac{1}{2\pi\sqrt{L_S C_S}} \tag{1}$$

The resonance frequency changes in response to pressure, and it can be detected by inductive telemetry with an external coil antenna. Through inductive coupling, the external coil energizes the sensor circuit, which provides a load impedance that is reflected back to the external coil. Reflected impedance, X_l, can be found as a function of the sensor impedance, Z_S, and the mutual inductance, M, between the external coil antenna and the integrated inductance in the sensor, as

$$X_l = \frac{(\omega M)^2}{Z_S(\omega)} \tag{2}$$

where

$$M = k\sqrt{L_e L_S} \tag{3}$$

$$Z_S(\omega) = R_S + j\left(\omega L_S - \frac{1}{\omega C_S}\right) \tag{4}$$

where ω is the angular frequency, k the coupling coefficient, and L_e the inductance of the external coil. The impedance seen at the external coil due to coupling is given by [9,10]:

$$Z_e(\omega) = R_e + j\omega L_e + \frac{(\omega M)^2}{Z_S(\omega)} \tag{5}$$

where R_e and L_e are the series resistance and the inductance of the external coil, respectively. At the resonant frequency of the LC tank circuit, the impedance Z_S becomes purely resistive and reduces to only R_S, therefore, the impedance of the external antenna becomes

$$Z_e(\omega_0) = R_e + j\omega_0 L_e + \frac{(\omega_0 M)^2}{R_S} \tag{6}$$

By monitoring the overall impedance change of the external coil due to the reflected impedance, it is possible to detect the sensor resonance frequency. This change is more detectable if the phase of Z_e is monitored. The approximate magnitude of the impedance phase dip is given by

$$\Delta\varphi_{DIP} \cong \tan^{-1}\left(\frac{\omega_0 M^2}{L_e R_S}\right) \tag{7}$$

The impedance phase dip is maximized when the series resistance of the electroplated coil, i.e. R_S, is minimized and its inductance, L_S, is maximized for larger M. However, it is important to note that, when L_S is increased by increasing the number of turns in the coil, then the parasitic capacitance of the coil also increases, decreasing the self resonant frequency of the planar coil [9,10]. The coil self-resonant frequency should be much higher than the operating frequency for proper device operation. It is also important to decrease the series resistance of the electroplated coil for a

more accurate detection of the resonant frequency of the sensor. Low-resistance (thus high Q) inductors can be implemented by depositing thick metal films with low specific resistivity. Copper electroplating, using a thick photoresist as a mold, proves to be the ideal candidate for this [6,8]. The increase in the series resistance of the coil at high operation frequencies due to skin effects should also be considered.

The planar inductor is modeled by L_S representing the series inductance and R_S representing the series parasitic resistance having frequency dependence related to the skin effect. The inductance of an air-core rectangular planar inductor can be calculated as [9]:

$$L_0 = 0.02339N^2$$
$$\times \left[(s_1 + s_2)\log\left(\frac{2s_1 s_2}{ND}\right) - s_1\log(s_1 + g) - s_2\log(s_2 + g)\right]$$
$$+ 0.01016N^2\left[2g - \frac{(s_1 + s_2)}{2} + 0.447ND\right]$$
$$- 0.01016N(s_1 + s_2)(A + B) \tag{8}$$

Series resistance of the inductor including skin effect can be calculated by [10]

$$R = \frac{\rho l}{w\delta(1 - e^{-h/\delta})} \tag{9}$$

$$\delta = \sqrt{\frac{2}{\omega\mu\sigma}} \tag{10}$$

where ρ is the resistivity, l the length of the coil, w the line width, h the height of the winding, δ the skin depth, ω angular frequency, μ the magnetic permeability of the core material, and σ is the conductivity of the coil material. Fig. 4 shows the simulation result showing skin depth and coil series resistance as a function of frequency. As the frequency increases, the skin depth decreases and thus the parasitic series resistance increases. The increase of parasitic resistance makes sensor detection more difficult.

Considering all of these parameters, a wireless pressure sensor is designed to operate in the 0–50 mmHg range with respect to ambient pressure. Table 1 summarizes the sensor characteristics and expected performance parameters.

Table 1
Summary of the wireless pressure sensor characteristics

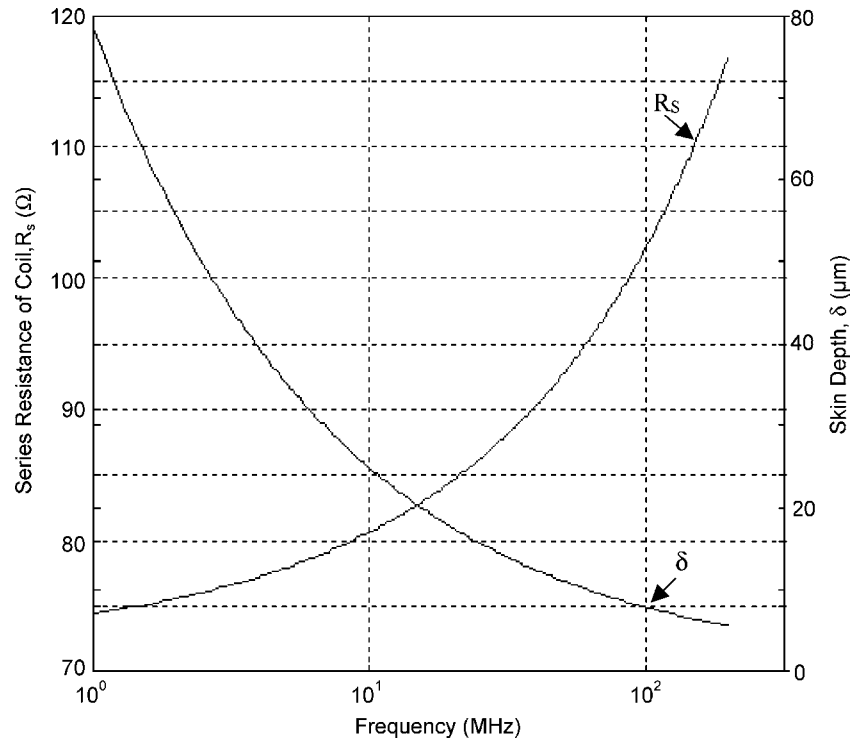| Parameter	Value
Diaphragm thickness (μm)	6
Capacitor plate separation (μm)	2
Full scale deflection (μm)	0.4
Dynamic range (mmHg)	0–50
Total diaphragm area	2 × (680 μm × 680 μm)
Device size	2.6 mm × 1.6 mm
Inductance (μH)	1.2
Capacitance change for 0–50 mmHg (pF)	2.0–2.35
Frequency shift for 0–50 mmHg (MHz)	103–95
Pressure sensitivity (ppm/mmHg)	1553
Pressure responsivity (kHz/mmHg)	160

Fig. 4. The simulation of skin depth and the coil series resistance chance as a function of frequency.
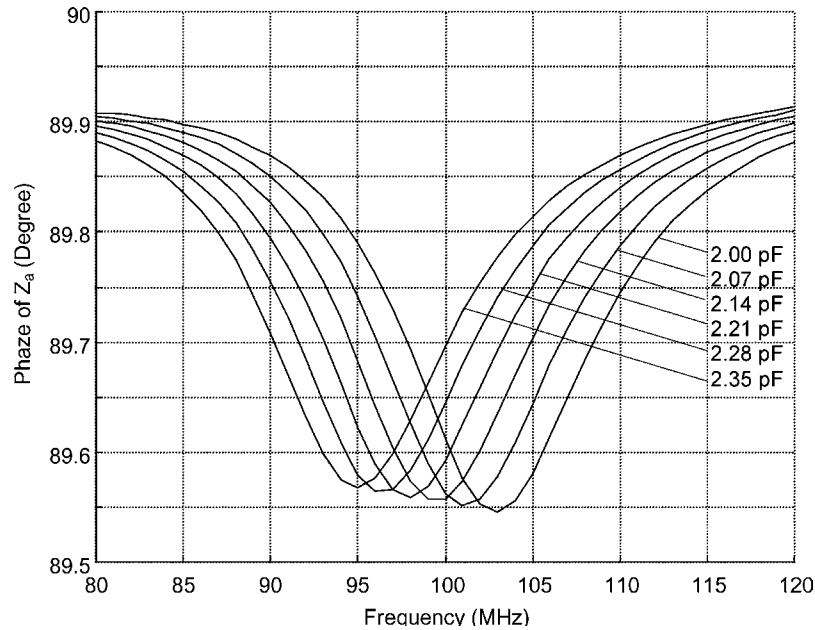

Fig. 5. Phase change in the exciting antenna coil due to change of the wireless pressure sensor resonant frequency.

Fig. 5 shows the simulated phase change on the exciting antenna coil due to change of the wireless pressure sensor resonant frequency. The resonant frequency changes from 103 to 95 MHz due to capacitance change from 2 to 2.35 pF. These values correspond to a pressure sensitivity of 1553 ppm/mmHg and a pressure responsivity of 160 kHz/mmHg. It is possible to obtain higher pressure sensitivity and responsivity with larger device dimensions.

4. Fabrication process

The fabrication process of the wireless capacitive pressure sensor is based on the bulk silicon dissolved wafer process [11] with some additional steps needed to integrate the on-chip electroplated coil. Fig. 6 shows the fabrication process steps for the sensor. A silicon wafer is selectively etched with KOH to create a 2 μm recess to define the capacitive
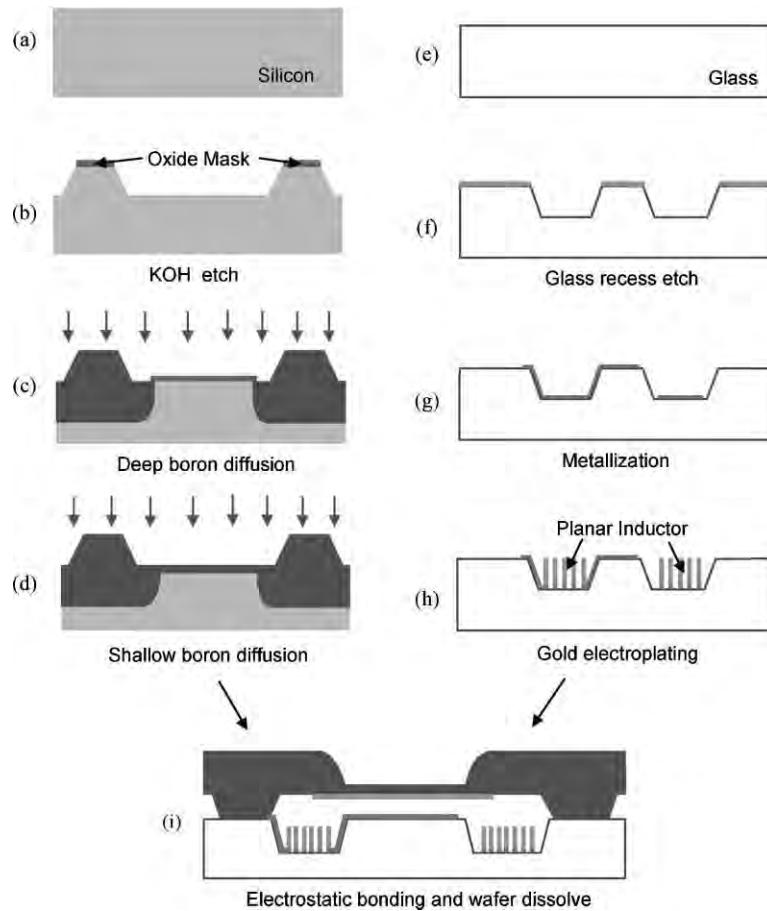
Fig. 6. Fabrication process for the wireless capacitive pressure sensor. (a) Silicon; (b) KOH etch; (c) deep boron diffusion; (d) shallow boron diffusion; (e) glass; (f) glass recess etch; (g) metallization; (h) gold electroplating; (i) electrostatic bonding and wafer dissolve.

gap (Fig. 6b). Then, two high-temperature boron diffusion steps are performed to define heavily doped p^{++} ($>7 \times 10^{19}$ cm^{-3}) region of 12 µm thick support anchors and the 3–6 µm thin diaphragm of the pressure sensor, respectively (Fig. 6c and d). The diaphragm thickness can be reduced down to 2.5 µm if necessary. A thin silicon

dioxide protection layer is then grown on the diaphragm. This thin oxide layer is used to prevent a short circuit if the diaphragm touches the bottom plate under large applied pressure. Meanwhile, a glass wafer is selectively etched to create a 7 µm recess (Fig. 6f) for the electroplated coil so that 6 µm-thick coil does not touch to the diaphragm of the
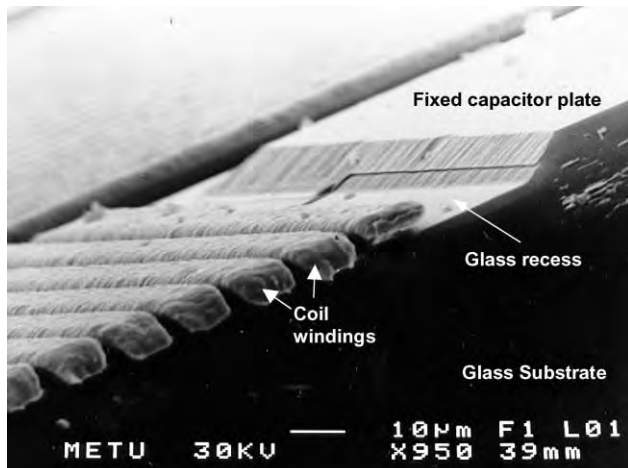

Fig. 7. SEM photograph of the gold electroplated coil windings.

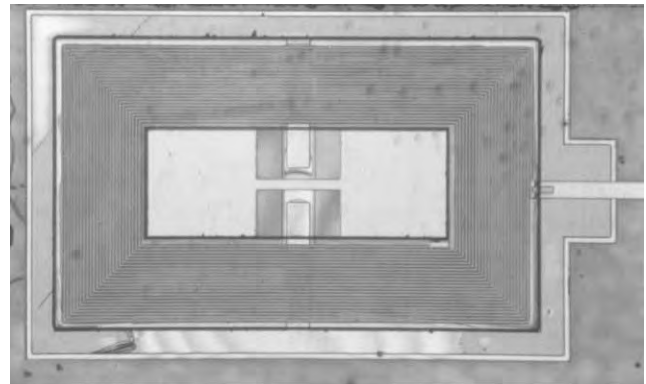Fig. 8. Photograph of a fabricated sensor seen through the glass substrate. This device measures 2.6 mm × 1.6 mm and supports a 24-turns gold-electroplated coil. The capacitive plate is separated into two parts to increase the dynamic range.
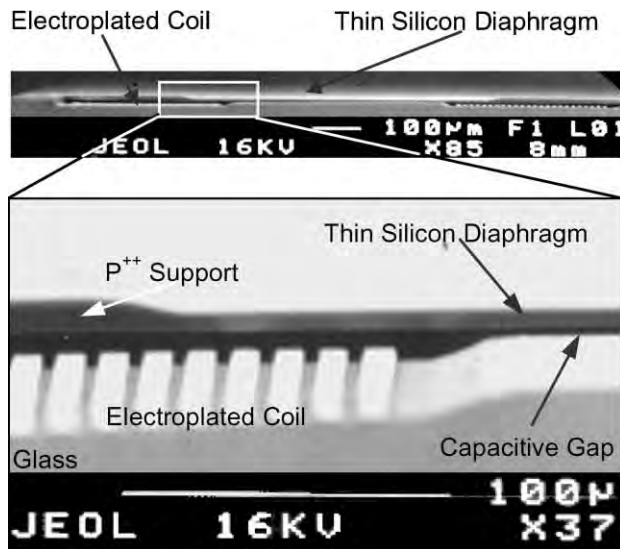
Fig. 9. SEM photograph of a fabricated sensor showing the cross-sectional view.

Fig. 10. Another SEM photograph of the fabricated sensor, which is broken to show the electroplated coil windings inside the sealed cavity.

capacitive pressure sensor. Then, a triple-layer metallization (Ti/Pt/Au) is deposited and patterned to form the fixed plate of the capacitor and the seed layer needed for electroplating on the glass wafer (Fig. 6g). The Ti/Pt layer provides good adhesion for metallization on the glass substrate.

The inductor structure is electroplated through a thick photoresist mold (Fig. 6h). The processed silicon and glass wafers are bonded together using anodic bonding to form the pressure sensor structure, and finally the lightly-doped bulk silicon is dissolved in ethylene–diamine–pyrocatechol–water solution (Fig. 6i).

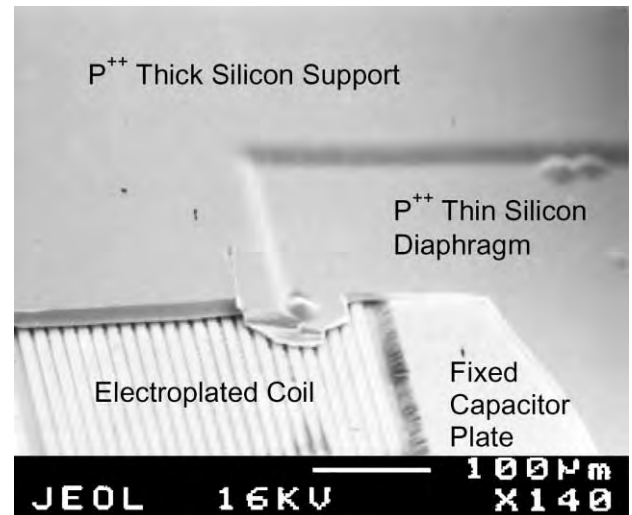This process has a number of advantages. It is a simple, batch, and high yield, and eliminates problems associated with discrete coil attachment. The coil is sealed inside the pressure sensor cavity, so that the harsh external environment does not affect it. It should be noted that for biomedical applications, all the materials used in this process are biocompatible, there is no need for additional protective coatings.

5. Fabrication and test results

A number of different sensor structures have been designed and fabricated. Fig. 7 shows an SEM photograph of the gold electroplated coil windings on the glass substrate
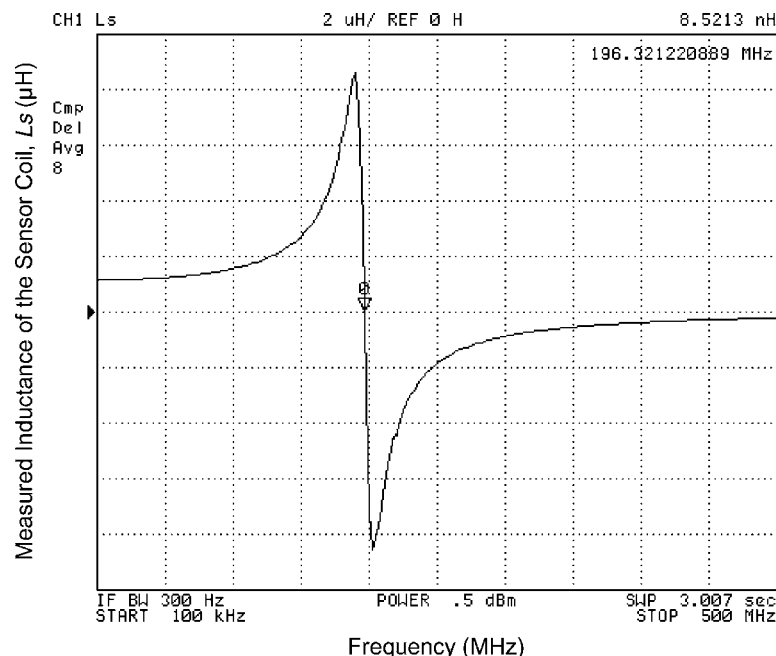

Fig. 11. The measured inductance characteristic of the electroplated coil, where the self-resonance frequency of the coil is 196 MHz.
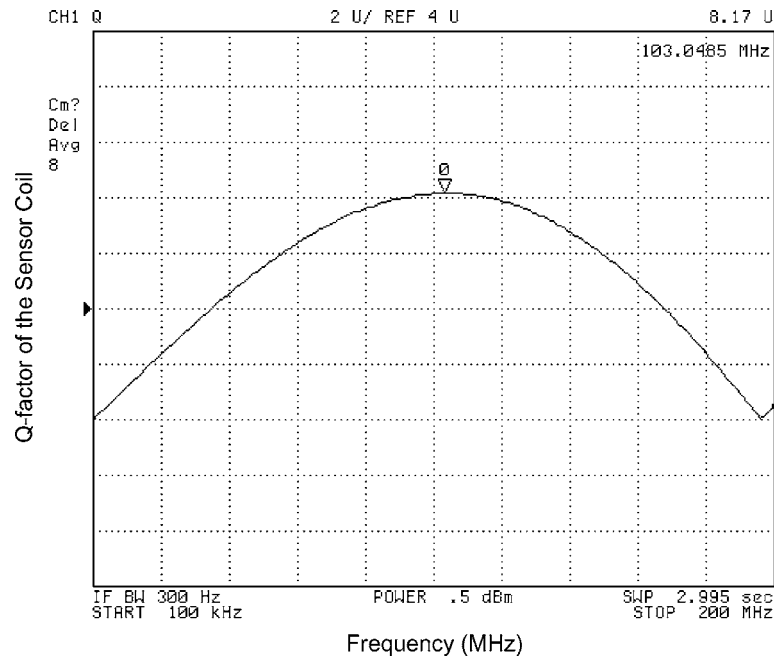
Fig. 12. *Q* of the coil, which increases up to its maximum of 8 at 103 MHz, i.e. around the designed operation frequency.

of one of the sensors. The width and height of the gold lines are 7 and 6 μm, respectively, while the separation of the lines is 7 μm. Fig. 8 shows a fabricated sensor seen through the glass substrate. This device is optimized for a pressure range of 0–50 mmHg, and it measures 2.6 mm × 1.6 mm supporting a 24-turns gold-electroplated coil. Fig. 9 shows the SEM photograph of the fabricated sensor showing the cross-sectional view of the capacitive gap, electroplated coil

windings, and heavily doped p^{++} silicon layer of diaphragm and support rim. Fig. 10 shows another SEM photograph of the fabricated sensor, which is broken to show the electroplated coil windings inside the sealed cavity.

The inductance of gold electroplated coils is measured to be 1.2 μH as designed. The inductor self-resonance frequency is also measured to verify that it is higher than the sensor operating frequency. Fig. 11 shows the measured
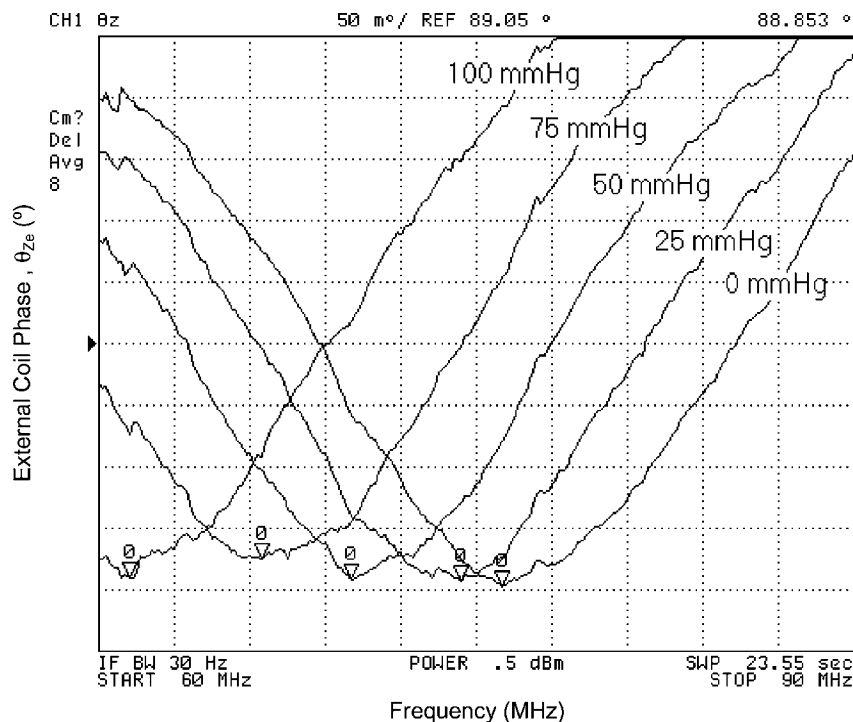

Fig. 13. External coil phase shift due to the resonant frequency shift of the sensor with the applied pressure.

inductance characteristic of the electroplated coil, where its self-resonance frequency is 196 MHz. Fig. 12 shows the Q of the coil, which increases up to its maximum of 8 at 103 MHz, i.e. around the designed operation frequency. These measurements show that the self-resonance frequency of the coil is higher than the sensor operation frequency, and the Q value of the coil is adequate. The Q of the coil can be increased if a lower resistance metal, such as copper, is electroplated instead of gold and if the thickness of the coil is increased by using a thicker photoresist mold.

A number of measurements were performed to verify the operation of the capacitive pressure sensor and to characterize its performance. The measurements were completed using a hand wound external coil, a pressure chamber, and an impedance analyzer. The hand wound solenoid coil was formed using a 0.38 mm diameter insulated copper wire. The coil had a diameter of 3 mm and 10-turns. The sensor in the chamber is placed above the external coil, so that planar sensor coil and the external coil are on the same axes with separation distance of about 2 mm. In the measurements, it was observed that the detection of the sensor resonance frequency is very sensitive to relative position of the coils due to low Q-factor of the sensor coil. Therefore, the detection of the phase chance due to resonance frequency change becomes more difficult. This can improved by increasing the Q of the coil as described above.

The phase shift on the external coil due to inductive coupling is monitored using HP 4395A Network/Impedance Analyzer. Fig. 13 shows the measured impedance phase changes in the external stimulating coil at different pressure values with respect to ambient pressure. The monitored resonant frequency change is between 76 and 70 MHz in the 0–50 mmHg pressure range, resulting in a pressure
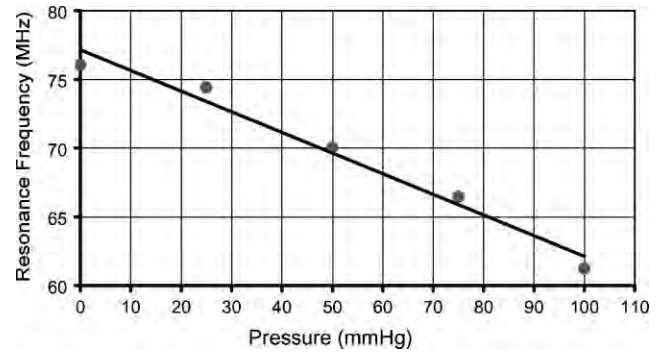

Fig. 14. Resonant frequency change of the sensor with the applied pressure with respect to the ambient pressure.

responsivity of 120 kHz/mmHg and a pressure sensitivity of 1580 ppm/mmHg. Fig. 14 shows remotely detected sensor resonance frequency change with respect to the applied pressure change from zero pressure to the over pressure value of 100 mmHg.

It should be noted here that the resonant frequency of the sensor seems lower than the design value when the simulation results in Fig. 5 is compared with the measurement results in Fig. 13. The reason is believed to be the difference between the actual pressure inside the cavity and the ambient pressure. The pressure in the cavity is not ambient pressure, but the applied pressure is monitored with respect to the ambient pressure. The pressure inside the cavity is lower than the ambient pressure, since during the anodic bonding process, the structure is heated up to 400 °C. When the device cools down, the air inside the sealed cavity contracts and pulls the diaphragm closer to the fixed metal capacitor plate on the glass, increasing the zero pressure capacitance, hence, decreasing the resonant frequency of the sensor.
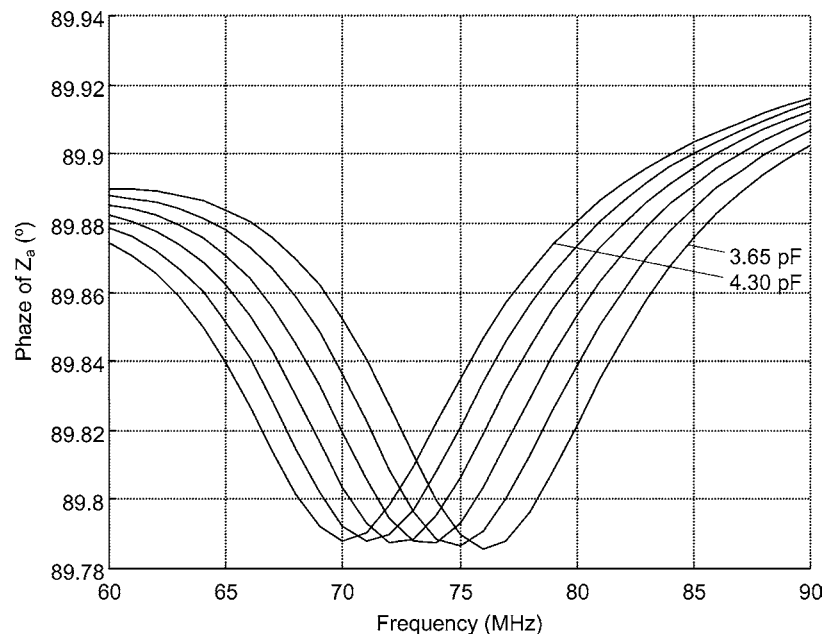

Fig. 15. The simulated impedance phase changes on the external stimulating coil related to the measured values, suggesting that the capacitance variation is between 3.65 and 4.3 pF.

Based on the measured zero pressure capacitance, simulations were repeated to determine sensitivity. Fig. 15 shows the simulated impedance phase changes on the external stimulating coil, suggesting that the capacitance variation is between 3.65 and 4.3 pF. Although the measured resonant frequency is different than the designed resonant frequency, the measured pressure sensitivity of the device is 1580 ppm/mmHg, which is very close to the design sensitivity of 1550 ppm/mmHg. The device sensitivity can be increased by increasing the device dimensions.

These measurements show that the device is functional and allows measuring the pressure of a sealed capacitive pressure sensor remotely, without requiring lead transfer from the sealed cavity.

6. Conclusions

An absolute wireless capacitive pressure sensor has been designed and fabricated. The sensor consists of a pressure sensitive capacitor and an integrated inductor forming a pressure sensitive resonant circuit. The resonance frequency of the sensor is measured by inductive telemetry. Fabricated devices measure $2.6 \, \text{mm} \times 1.6 \, \text{mm}^2$ in size and are optimized to provide a dynamic range of 0–50 mmHg. The fabricated device is operational, and its resonant frequency changes between 76 and 70 MHz when a pressure difference between 0 and 50 mmHg is applied across the diaphragm. This corresponds to a pressure responsivity and sensitivity of 120 kHz/mmHg or 1580 ppm/mmHg, respectively. Future work will focus on improvement of external detection system and fabrication of sensor coils with high Q-factor, so that the system will have a larger operation distance and a better tolerance to alignment mismatches.

Acknowledgements

References

[1] A. Chavan, K.D. Wise, A batch-processed vacuum-sealed capacitive pressure sensor, Tech. Digest, in: Proceedings of the 9th International Conference on Solid-State Sensors and Actuators (TRANSDU-CERS'97), Chicago, USA, 16–19 June 1997, pp. 1449–1452.

[2] R. Puers, Linking sensors with telemetry: impact on the system design, Sens. Actuat. A 52 (1996) 169–174.

[3] B. Ziaie, M.D. Nardin, A.R. Coghlan, K. Najafi, A single-channel implantable microstimulator for functional neuromuscular stimulation, IEEE Trans. Biomed. Eng. 44 (1997) 909–920.

[4] W.N. Carr, S. Chamarti, X. Gu, Integrated pressure sensor with remote power source and remote readout, Tech. Digest, in: Proceedings of

the 8th International Confernce on Solid-State Sensors Actuators (TRANSDUCERS'95) Eurosensors IX, Stockholm, Sweden, 25–29 June 1995, pp. 624–627.

[5] J.M. English, M.G. Allen, Wireless micromachined ceramic pressure sensors, Tech. Digest, in: Proceedings of the 12th IEEE International Conference on Micro Electro Mechanical Systems (MEMS'99), Orlando, FL, USA, 17–21 January 1999, pp. 511–516.

[6] E.-C. Park, J.-B. Yoon, E. Yoon, Hermetically sealed inductor–capacitor (LC) resonator for remote pressure monitoring, Jpn. J. Appl. Phys. 37 (1998) 7124–7128.

[7] T. Harpster, S. Hauvespre, M. Dokmeci, K. Najafi, A passive humidity monitoring system for in-situ remote wireless testing of micropackages, in: Proceedings of the 13th IEEE International Conference on Micro Electro Mechanical Systems (MEMS 2000), Miyazaki, Japan, 22–27 January 2000.

[8] R.S. Jachowicz, G. Wojtowicz, J. Weremczuk, A non-contact passive electromagnetic transmitter to any capacitive sensor—design, theory, and model tests, Sens. Actuat. A 85 (2000) 402–408.

[9] F.E. Terman, Radio Engineer's Handbook, McGraw-Hill, New York, 1943.

[10] E.G. Weber, Inductance magnetic materials, in: K. Henney (Ed.), Radio Engineering Handbook, McGraw-Hill, New York, 1959.

[11] H.L. Chau, K.D. Wise, An ultraminiature solid-state pressure sensor for a cardiovascular catheter, IEEE Trans. Electron Dev. 35 (12) (1988) 2355–2362.

Biographies

Orhan Akar was born in Samsun, Turkey, in 1972. He earned his BS degree in electronics and communication engineering from Istanbul Technical University in 1994 and MS degree in electrical and electronics from Middle East Technical University in 1998. From 1996–2001 he was employed as a research engineer in VLSI Design Group at TUBITAK-BILTEN. He is also a member of METU-MEMS Research Group since 1996. His research interests include the implementation of MEMS, silicon micromachining, capacitive pressure sensors.

Tayfun Akin was born in Van, Turkey, in 1966. He received the BS degree in electrical engineering with high honors from Middle East Technical University, Ankara, in 1987 and went to the USA in 1987 for his graduate studies with a graduate fellowship provided by NATO Science Scholarship Program through the Scientific and Technical Research Council of Turkey (TUBITAK). He received the MS degree in 1989 and the PhD degree in 1994 in electrical engineering, both from the University of Michigan, Ann Arbor. Since 1995 and 1998, he has been employed as an assistant professor and associate professor, respectively, in the Department of Electrical and Electronics Engineering at Middle East Technical University, Ankara, Turkey. He is also the technical coordinator of METU-MET, an IC fabrication factory which is transferred to Middle East Technical University by the government for MEMS related production. His research interests include MEMS (Micro-Electro-Mechanical Systems), infrared detectors and readout circuits, silicon-based integrated sensors and transducers, and analog and digital integrated circuit design. He is the winner of the first prize in Experienced Analog/Digital Mixed-Signal Design Category at the 1994 Student VLSI Circuit Design Contest organized and sponsored by Mentor Graphics, Texas Instruments, Hewlett-Packard, Sun Microsystems, and Electronic Design Magazine. He is the co-author of the symmetric and decoupled gyroscope project which won the first prize award in the operational designs category of the international design contest organized by DATE Conference and CMP in March 2001.

Khalil Najafi was born in 1958. He received the BS, MS, and the PhD degree in 1980, 1981 and 1986, respectively, all in Electrical Engineering from the Department of Electrical Engineering and Computer Science, University of Michigan, Ann Arbor. From 1986–1988 he was employed as

a Research Fellow, from 1988–1990 as an assistant research scientist, from 1990–1993 as an assistant professor, from 1993–1998 as an associate professor, and since September 1998 as a professor and the director of the Solid-State Electronics Laboratory, Department of Electrical Engineering and Computer Science, University of Michigan. His research interests include: micromachining technologies, solid-state micromachined sensors, actuators, and MEMS; analog integrated circuits; implantable biomedical microsystems; hermetic micropackaging; and low-power wireless sensing/actuating systems. Dr. Najafi was awarded a National Science Foundation Young Investigator Award from 1992–1997, was the recipient of the Beatrice Winner Award for Editorial Excellence at the 1986 International Solid-State Circuits Conference, and of the Paul Rappaport Award for co-authoring the Best Paper published in the IEEE Transactions on Electron Devices. In 1994, he received the University of Michigan's "Henry Russel

Award" for outstanding achievement and scholarship, and was selected as the "Professor of the Year" in 1993. In 1998, he was named the Arthur F. Thurnau Professor for outstanding contributions to teaching and research, and received the College of Engineering's Research Excellence Award. He has been active in the field of solid-state sensors and actuators for more than 15 years, and has been involved in several conferences and workshops dealing with solid-state sensors and actuators, including the International Conference on Solid-State Sensors and Actuators, the Hilton-Head Solid-State Sensors and Actuators Workshop, and the IEEE/ASME Micro Electromechanical. Systems (MEMS) Workshop. Dr. Najafi is the editor for *Solid-State Sensors* for *IEEE Transactions on Electron Device*s, and associate editor for *IEEE Transactions on Biomedical Engineering*, and an associate editor for the *Journal of Micromechanics and Microengineering*, Institute of Physics Publishing.